GEOPHYSICAL IMAGING OF THE LIQUIÑE GEOTHERMAL SITE (39°S, CHILE) BY MEANS OF 3D GRAVITY INVERSION

Elizalde Daniel[1,2,*], Azócar Elena[1], Crempien Jorge G. F.[1,2], Arancibia Gloria[1,2], Molina Eduardo[1,2], Roquer Tomás and Pérez-Estay Nicolás[2,3]

[1] Departamento de Ingeniería Estructural y Geotécnica, Pontificia Universidad Católica de Chile, Av. Vicuña Mackenna 4860, Macul, Santiago, Chile.

[2] Centro de Excelencia en Geotermia de los Andes (CEGA, FONDAP-CONICYT), Universidad de Chile, Plaza Ercilla 803, Santiago, Chile.

[3] Departamento de Geología, Universidad de Chile, Plaza Ercilla 803, Santiago, Chile.

* Corresponding author: jdelizalde@ucl.cl

Keywords: *Geothermal resources, Geophysical method, Bouguer gravity inversion, Liquiñe, Chile.*

ABSTRACT

The Liquiñe geothermal site is characterized by an anomalous number of geothermal hot springs (with in-situ measured temperatures ranging between 35-75 °C), which are spatially related to the main NS lineaments of the Liquiñe-Ofqui Fault System (LOFS) and NW-SE Andean Transverse Faults (ATF). Country rocks are dominated by granitoids and scarce mylonitic gneisses. The lateral continuity of most of the mapped outcrops and structural elements are interrupted by dense vegetation and soil cover, which highlights the necessity to perform further geophysical campaigns aimed to constrain the structural control on thermal hot springs. In this work we present a gravimetric survey developed along the Liquiñe valley. NW-SE and N-S profiles, obtained in an area of ~36 km2, allowing us to define the subsurface morphology of the basement. To invert the Bouguer anomaly, we used the open source SimPEG software (https://simpeg.xyz/) to constrain a 3D density model within the extension of the gravimetric survey. Our results show two main Bouguer gravity anomalies were detected, the first one related to two main NS lineaments of the LOFS, which also correlates with the thermal spring manifestations within the Liquiñe village. This Bouguer anomaly is interpreted as the consequence of highly fractured rock zones, increasing permeability. The second major Bouguer gravity anomaly is related to a topographic relief, consistent with a recognized proximal ATF trace. An increase of the basin thickness from south to north, with a thickness of a ~10 m to a maximum of ~200 m, respectively. Furthermore, these observations are also supported with the 3D density model, for depths up to 300 m, which draws a picture of a complex three-dimensional structural system.

1. INTRODUCTION

A gravity method involves measuring the earth's gravitational field at specific locations on the surface to detect the locations of subsurface rock density variations (Harvey et al., 2016). It is one of the geophysical techniques used in geothermal exploration because the density can be affected by the temperature and fluid content within the rock (Árnason and Flóvenz, 1992). According to Glassley (2015), the interpretation of these changes in the density parameter can be difficult due to several factors: 1) the fluid's density which may fill fractures and/or pores, 2) the water-rock interaction, 3) mineral replacement, such as e.g., clay minerals and zeolites from feldspars, and 4) the fracturing degree of the rocks. Regarding the last point, fractured rocks related to fault zones are especially interesting because they can allow the developing of geothermal resources in crystalline rocks with low primary porosity (e.g. Mickelthwaite et al., 2010). The improvement of this secondary or structural permeability can be reached by the interaction between regional stresses (pressure), the thermal gradient (temperature), and the hydromechanical response (intrinsic properties) of the country rocks in tectonically active regions (Cox, 2010; Rowland and Simmons, 2012). However, in some cases these fractured zones may not be well exposed due to the fact that they are covered or even, they are not outcropping in surface. In these cases, when there are thermal manifestations but the architecture and arrangement of the fractured area through which the fluids circulate cannot be observed, geophysical techniques can be a fundamental tool to determine in depth how this resource is distributed or how it can be conditioned by structures (e.g. Meju, 2002; Muñoz, 2014).

The Liquiñe geothermal site is characterized by an anomalous amount of geothermal hot springs (with in-situ measured temperatures ranging between 35-75 °C), which are spatially related to the main NS lineaments of the Liquiñe-Ofqui Fault System (LOFS) and NW-SE Andean Transverse Faults (ATF). Exploration is being done at this site to characterize both fault systems, however, the lateral continuity of most of the mapped outcrops and structural elements are interrupted by dense vegetation and soil cover. Therefore, in order to take advantage of Liquiñe's geothermal resources, it is necessary to understand how its hydrothermal system works, and the characteristics of its different geological features. In the Liquiñe village, there are two superficial evidences of thermal activity at depth. First, most hot springs are spatially located above the main NS lineaments of the Liquiñe-Ofqui Fault System and NW-SE Andean Transverse Faults (e.g. Sánchez et al., 2013; Tardani et al., 2016). Second, hot springs occur at the valley boundary, where there is contact between sedimentary and igneous rocks. Both lateral and vertical depth information are needed to identify whether fluid circulation is controlled by geological structures and/or lithological contacts and the geometrical relationships between them.

The aim of this study is to improve the knowledge of identified lineaments from satellite images and associated structures at depth, and additionally, to identify the structural controls on hot springs related to both LOFS and ATF. This is a difficult task due to the interruption of the visibility of lateral continuity of most of the mapped outcrops and structural elements, which are interrupted by dense

vegetation and soil cover. To detect the structures of interest, we developed a gravimetric survey in an area of ~36 km^2 by means of three NW-SE and one N-S profiles of Bouguer anomaly. The results were interpreted i) bouguer anomaly shape, ii) sedimentary thickness or basement geomorphology estimated from a residual gravity anomaly, and finally iii) the 3D density model obtained by the inversion of the Bouguer anomaly.

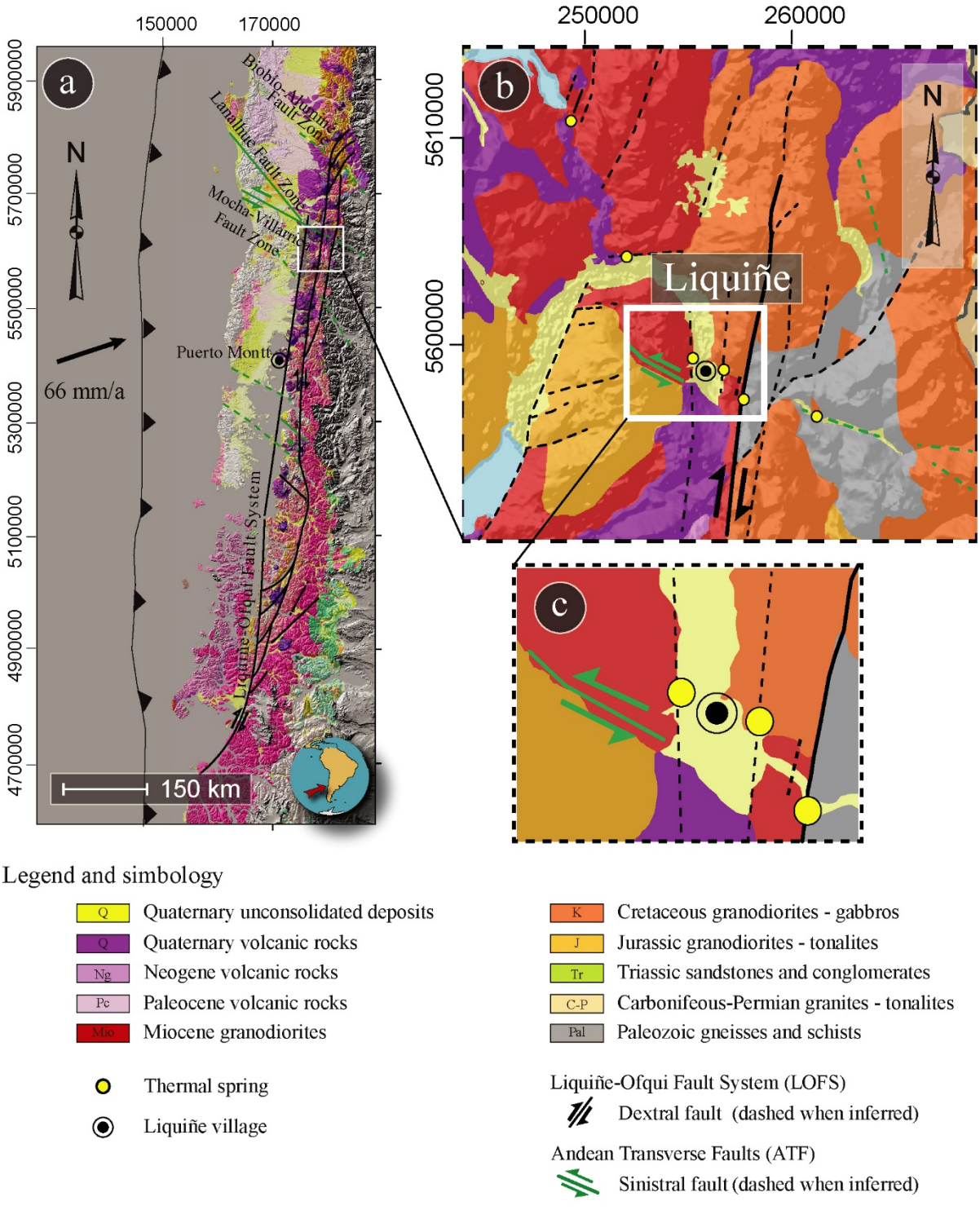

Figure 1: a) Tectonic framework of the Southern Volcanic Zone of the Andes (SVZ) (33°S-46°S). b) Local geological context of the Liquiñe Geothermal Site (LGS) and the study area is located on the white rectangle (c). Modified from Lara and Moreno (2004), Rosenau et al. (2006) and Sánchez et al. (2013).

2. GEOLOGICAL SETTING

In the Southern Volcanic Zone (SVZ) (33-46ºS), the partition of deformation produced by the subduction of the Nazca plate under the South American plate, is accommodated into orthogonal and parallel to the trench components. From these two components, the regional tectonic setting is characterized by the arc-parallel Liquiñe–Ofqui fault system (LOFS) and Andean Transverse Faults (ATF). Both are active and long-lived regional scale groups of faults (Fig. 1-a) (e.g. Cembrano et al., 1996; Rosenau et al., 2006). LOFS is an intra-arc dextral-slip fault system dominated by NS to NNE-striking master faults (Melnick et al., 2006; Cembrano and Lara 2009), and ATF's are a family of NW to WNW striking continental-scale lineaments (e.g. Pérez-Flores et al., 2016). The magmatic (volcanoes and minor eruptive centers) and hydrothermal fluids (thermal springs) are apparently controlled and favored by the LOFS and ATF's, because they play a first-order role in the transmission or storage of fluids as suggested in recent studies (e.g. Sánchez et al., 2013; Pérez-Flores et al., 2016; Tardani et al., 2016; Wrage et al., 2017; Held et al., 2018).

As a case study, we selected the Liquiñe area (39ºS) (Fig. 1-b and c), which is located in the Los Ríos region (southern Chile), between the geographical coordinates 39°42'34'' and 39°45'36'' south latitude and 71°53'21'' and 71°49'39'' west longitude. The area is placed in a wide river valley with a flat bottom and the current flowing through the valley comes from the Liquiñe River and other tributaries rivers. The dominant vegetation in the valley corresponds to a temperate rainforest (Luebert and Pliscoff, 2006). These forests are characterized by dense vegetation and bushes, which make them virtually impenetrable. Due to this, there are few visible rock outcrops along the proximity of slopes of Route 201 by the constant rehabilitation.

The study area is hereby referenced as "Liquiñe geothermal site" (LGS) due to the high amount of hot spring manifestations. These hot springs are spatially related to both main groups of faults (LOFS and ATF) and mainly upwelling from unconsolidated (alluvial and/or glacial) deposits overlying granitoids and metamorphic rocks (Sánchez et al., 2013; Tardani et al., 2016; Wrage et al., 2017; Held et al., 2018). These authors showed that these hot waters present a meteoric geochemical signal, with estimated temperature of potential reservoirs between 80 to 160 ºC, indicating that this corresponds to a low- to medium-enthalpy geothermal system. The Paleozoic metamorphic basement and Jurassic to Miocene granitoids of the North Patagonian Batholith (Munizaga et al., 1988) are cut by both groups of faults, and the area is locally covered by Paleocene to Neogene volcanic rocks and the Quaternary unconsolidated sediments (Lara and Moreno, 2004).

3. METODOLOGY

3.1 Gravity survey

The gravity survey was carried out with a CG5-Syntrex gravimeter. From the measurements, instrumental drift and the effect of luni-solar attraction (gravimetric tide) where automatically removed. Furthermore, we used a Trimble-Differential GPS to determine precise elevation above sea level. The differential GPS data were processed with the Panguipulli base station, ~40 km away from our site (Centro Sismológico Nacional de Chile).

Four profiles were designed to cover the LGS area and check for lateral changes in both N-S and NW-SE faults. In this way 3 profiles were made with NW-SE orientation and one N-S orientation. Based on this design, the distribution of 145 observation points as shown in Fig. 2. The point density is conditioned by the accessibility, such as public roads, so the density is highest within the Liquiñe village. The contrast is on the banks of the valley due to the amount of vegetation which affected to the quality of the GPS signal, and, the access can be difficult, either by abrupt elevations of the terrain and/or the inability to access private land.

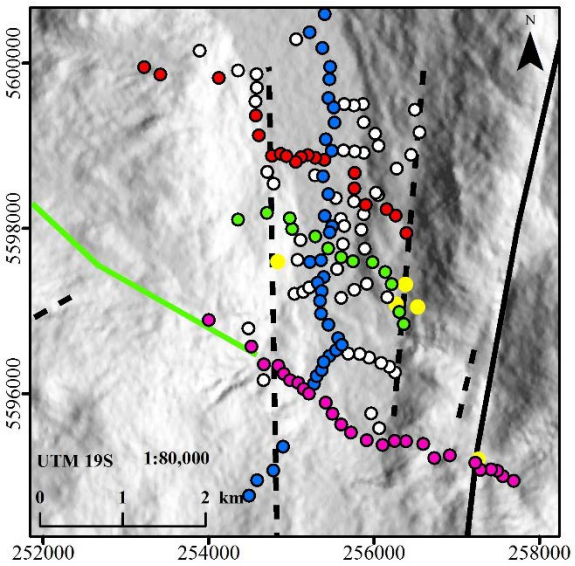

Figure 2: Spatial distribution of the survey stations and profiles. The selected NW-SE profiles are AA' (red), BB' (green) and DD' (purple). The N-S profile is EE' (dark blue). White dots were not considered for the profiles. LOFS (black) and ATF (green) structures and lineaments are drawn as continuous and discontinuous line, respectively. The hot springs are indicated with yellow dots.

3.2 Data processing

3.2.1 Bouguer anomaly

The calculation of Bouguer anomaly was performed as follows (Blakely, 1995): 1) the observations of gravity relative to a gravimetric referenced point in Pucon village (71°58'45" W, 39°16'33"S) were linked to obtain absolute values of gravity (Nettleton, 1971); 2) the acceleration of gravity due to the average mass, shape and rotation of the planet at the measurement site and the gravity due to the material underlying the area under study were subtracted from the absolute observations (2670 kg/m^3); 3) topography was considered to correct its effect on gravity. The residual effect of the Bouguer anomaly was estimated as the contribution and was separated by the regional geological effects, such as the root of the Andes range. 4) Finally, the Bouguer anomaly was represented in profiles in order to know the effect of the distribution of density in the rocks of the subsoil of the LGS.

3.2.2 Sedimentary basin thickness

We calculated the residual anomaly related with the sedimentary thickness subtracting a regional Bouguer tendency (as a plane) to the Bouguer anomaly. Regional tendency is related with geological effects, such as the root of the Andes range (e.g. Tassara and Yañez, 2010).

The sedimentary basin thickness was estimated with the eq. 1. For that, an infinite density plate was assumed to obtain:

$$h = \frac{\Delta g}{2\pi G \Delta \rho} \qquad \text{eq. 1}$$

Where "h" is the sedimentary thickness (in m), Δg is the residual anomaly (in mGal), G is the universal gravity constant 6.674×10^{-11} $N\times m^2/kg^2$ and Δρ is the density contrast between the sediments and the basement, in this case estimated as 670 kg/m^3.

3.2.3 Gravity inversion

To invert the Bouguer anomaly we used the open source SIMPEG (Simulation and Parameter Estimation in Geophysics) (Cockett et al., 2015) and software to build a 3D density model within the extension of the gravimetric survey.

According to Miller et al. (2017) we follow their procedure because they found that SimPEG does a mixed Lp norm inversion on both model values, and the gradient of their distribution, to obtain a better simulation of the geologic models with sharp or gradational boundaries according to the user´s preference.

4. RESULTS

Profiles A-A', B-B' and D-D' were chosen to describe the behavior of Bouguer anomaly because they are perpendicular to NS lineaments (Fig. 2). Bouguer anomaly values range from -56 mGal to -68 mGal (Fig. 3). The highest values (-56 mGal) mean that below this point, the density distribution surrounding this point is higher, resulting in a positive contrast. On the contrary, values around -68 mGal mean a negative contrast if the density of the point is lower than that of the environment. In this way, Figure 4 shows a positive lateral contrast towards the eastern and western border of the valley where there are granite rocks, and negative in the valley (Fig. 1-c and Fig. 2). In relation to the NS lineaments, all the profiles show a negative anomaly close to these lineament, which have higher or lower amplitudes (between XX and YY mGal). In the case of D-D' profile, it is also observed on the east side of the area, the effect of other minor lineaments and a more marked effect of a main trace (continuous black line) of the LOFS.

From the residual values of the Bouguer anomaly (Fig. 4 upper profile) of the E-E' profile and the contrast of density between the igneous and sedimentary rocks (assumed to be 670 kg/m^3) observed that the sedimentary thickness increases from the south to north of the valley. The calculated thickness varies from ~10 m (South) to a maximum of ~200 m (North) (Fig. 4, bottom profile).

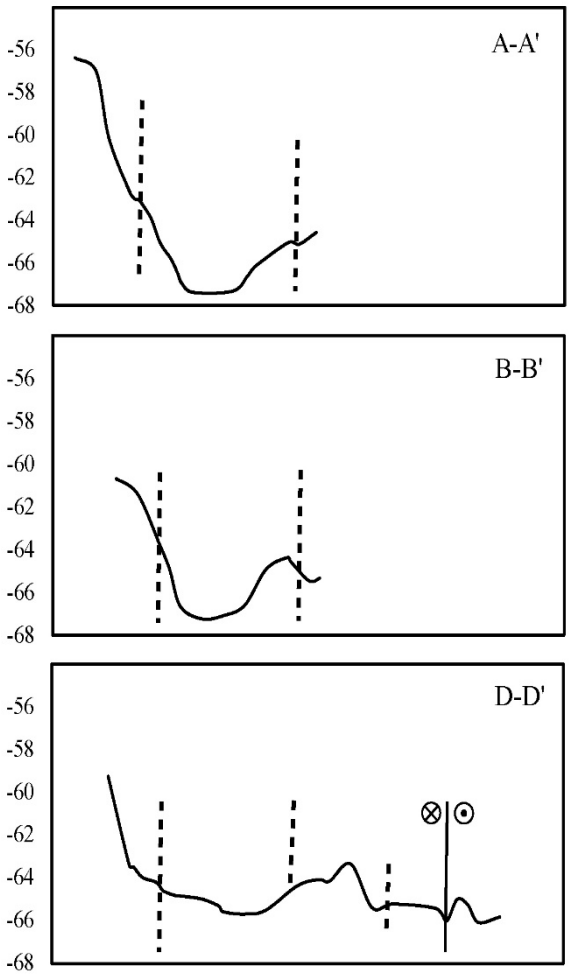

Figure 3: NW-SE Bouguer anomaly profiles. Vertical axis is Bouguer anomaly in (mGal) and horizontal axis represents the distance. The position of AA', BB' and DD' profiles are indicated in Figure 2.

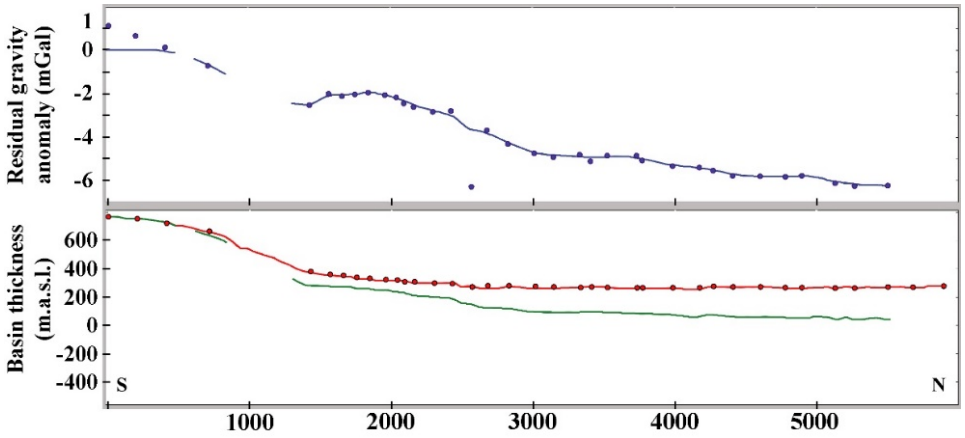

Figure 4: Basin thickness of the Liquiñe valley. Upper profile is the residual gravity anomaly (mGal). Blue dots are the observed gravity anomaly. Blue line is the 1D modeled gravity anomaly (equation 1). Bottom profile is basin thickness

(m.a.s.l.). Red line is the topography from a DEM with a pixel of 30 m. Green line is the modeled basin surface. Red dots are the differential GPS topography.

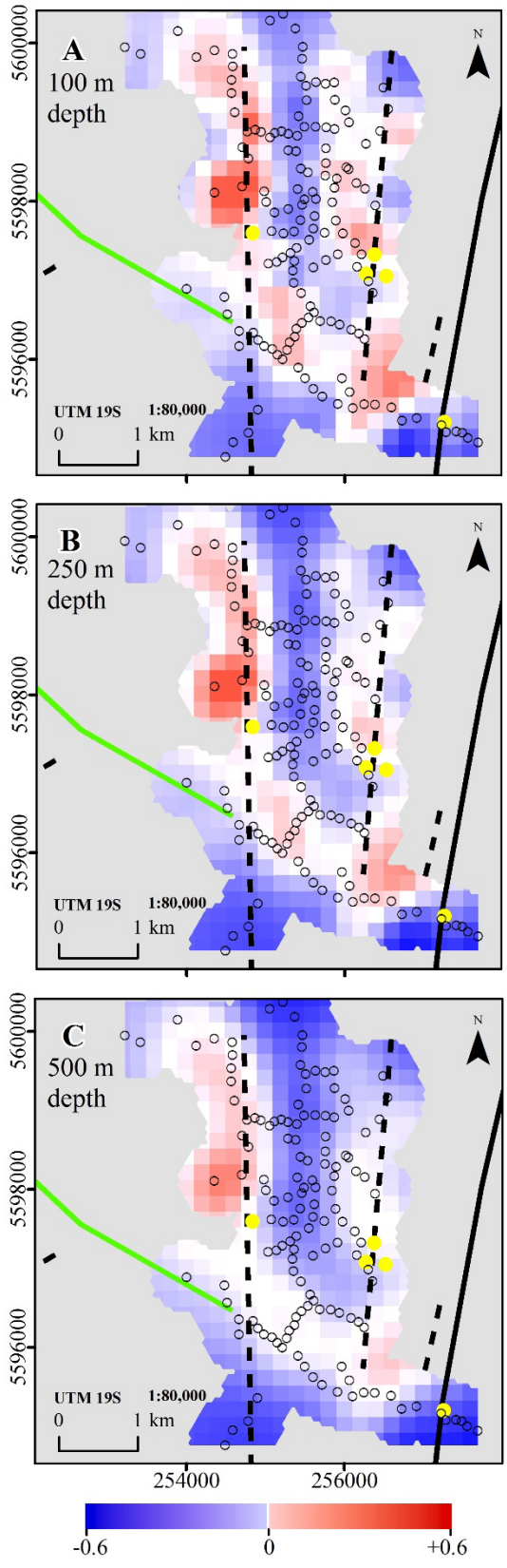

Figure 5: Gravity inversion under topography A: 100 m depth, B: 250 m depth and C: 500 m depth. Units of the color bar express density contrast (in g/cm^3)

and circles are gravity observations. LOFS (black) and ATF (green) structures and lineaments are drawn as continuous and discontinuous line, respectively. The hot springs are indicated with yellow dots.

From the inversion of the Bouguer anomaly, an image was obtained of the contrast of density in the subsoil at depths of 100 m, 250 m and 500 m (Fig. 5 a-c). The contrast is positive or negative if the density is greater or less than 2670 kg/m^3, respectively. It was observed that from the first 100 meters down to 500 m depth the behavior of the density is relatively constant, so the geometry of the contours and the area are comparable. Three main positive contrast are observable: two N-S trending direction along the segmented line which represent main geomorphological lineament of the area restricting the valley (Fig. 5 a-c); and one NW trending as the continuity of the green line which represent one of the ATF observed in one outcrop. Negative anomalies are concentrated in the edge of the area, and the most important anomaly it has a NS trending direction in the center of the Fig. 5, where the valley and the sedimentary basin occur. Therefore, these positive contrasts are related to the described lineaments and mapped faults, especially related to LOFS, and with less resolution with the ATF observed in the south of the area.

5. DISCUSSION

A gravity survey was carried out as a first approximation to locate structures that were previously only inferred from the lineaments observed from satellite images and evidences in the field. These structures must be usually inferred because the area is practically covered by vegetation. Figure 6 shows the distribution of the vegetation, where white areas correspond to forest and grey areas covered by bare soil and/or slightly covered with grasslands and crops. As can be appreciated, in the studied area there is not any pixel with exposed rock outcrop, at least, at the resolution level used in the processed image, which is 30x30 m each pixel. Therefore, the use of geophysics, such as gravimetric survey, are a fundamental tool to complement the observations made in the outcrops that exist in this area.

With the Bouguer anomaly profiles (Fig. 3) it has been possible to confirm the position of the lineaments, for both the ATF and especially those related to LOFS. In this sense, a example is manifested in the effect produced in the anomaly by the main trace of LOFS (continue black line in figures 1, 2 and 5 at XX meters in profile DD of Fig. 3), recognized in the field (Cembrano et al., 2000), since it shows a marked decrease in values with respect to the adjacent recorded points (Fig. 3, DD' profile). This variation between points could also indicate a relative extension of the damage zone related to this fault, which could have an approximate width of less than 200 m. However, this aspect should be corroborated by measuring more points in the area to be able to confirm this effect of the trace with respect to the amount of damage (increased fractures) in the country rock. In addition, the inversion of Bouguer anomaly has also allowed to confirm these lineaments at depth by the contrast in density (Fig. 4), especially where the value of $\Delta\rho$ is ≈ 0. However, this contrast could be indicating two aspects to be considered for its interpretation, being (1) that mentioned contrast is due to the presence of two different lithologies (Fig. 1); and (2) this change in density is due to areas with a

higher percentage of fractures. These two options are not exclusive, since this effect is detected on the lateral borders of the valley, where the lineaments are located as well as the lithological contact between Miocene and Cretaceous granitic rocks and Quaternary unconsolidated sediments. From the 3D model (Fig. 5), it is also observed that both the position of the lineaments and the possible damaged zones are constant at least up to 500 m in depth. So, it would be indicating that they are elements with a marked verticality. Therefore, the lateral contrast in density at different depths could be indicating an increase in temperature or a high rock water content due to the presence of areas with greater fracture abundance, related to a fault damage zone (structural permeability). This effect about the contrast in density in highly fractured rock zones, with an increase of the permeability, was observed by other authors (Atef et al., 2016; Kryak et al., 2015, Djebbi and Gabtni, 2018). So, these characteristics could possibly favor the circulation to depth of cold waters and the thermal fluids rising towards the surface. On the other hand, the amount of interconnected fractures could justify the position of the hot springs, appearing where this value is high; while those fractured areas but with a lower degree of connection would not present thermal springs, even though it also has values of $\Delta\rho \approx 0$ (white pixels in fig. 5).

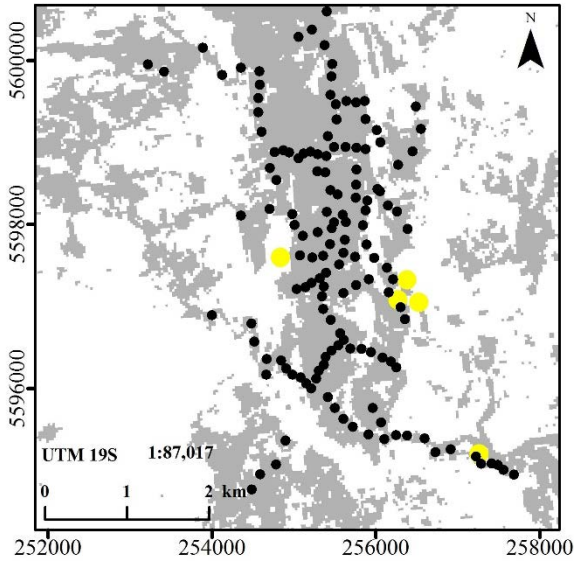

Figure 6: Processed Landsat 8 OLI satellite image using the near infrared and visible region to enhance spectral response of vegetation (in white) and the bare soil along with the urban area of Liquiñe (in dark grey). Black dots are the gravity observations and the yellow dots are the hot springs.

With respect to the thickness of the sedimentary material, it increases towards the North. This increase could be due to a greater subsidence of the basin in that sector and/or the effect on the variation of the accommodation space. With the data taken from gravimetry survey, at the moment, we cannot discern more about this aspect, but the presence and interaction of the ATF and LOFS faults to the south of the study area, could produce a tilting or a greater accommodation space to the north, favoring in this sense the accumulation of sediment in that direction. Finally, the concrete position of the hot springs, justified in relation to the lineaments and possible areas with a greater degree of interconnection of fractures, it has been observed that the sedimentary thickness towards the edges decreases, which would also facilitate the upwelling occurring at the borders of the valley. However, it cannot be ruled out that there are points with thermal upwellings in the valley, but based on everything discussed above, since the valley has the highest sediment thickness (very porous material), the effect of cold meteoric water would decrease the probability of finding these hot water points.

6. CONCLUSIONS

The main conclusions that have been obtained from this first gravimetric survey developed in the Liquiñe area are:

1) We have found some evidences to corroborate the position of the main lineaments of the LOFS and ATF identified from the satellite image and field outcrops, as well as their continuity throughout the study area and, at least, up to 500 m in depth.

2) The circulation of thermal fluids in the Liquiñe Geothermal Site would be controlled by the combination of the spatial position of the lineaments as well as the presence of areas with greater interconnection of fractures in the damage zone of these lineaments, and the lower sediment thickness overlaying fractured granitic rocks.

ACKNOWLEDGEMENTS

This work is a contribution to FONDAP-CONICYT Project 15090013 and it is funded by FONDECYT Regular project 1180167 and by Corporación Regional of Los Ríos Region. We also thank Karin García for her great support in data acquisition in the field campaign and Valeria Becerra for her programming support.

REFERENCES

Árnason, K., and Flóvenz, Ó.G.: Evaluation of physical methods in geothermal exploration of rifted volcanic crust. *Geothermal Resources Council, Transactions* 16. pp. 207 – 214. (1992).

Aretouyap, Z., Nouck, P., Nouayou, R.: A discussion of major geophysical methods used for geothermal exploration in Africa. *Renewable and Sustainable Energy Reviews* 58. pp. 775 – 781. (2016).

Blakely, R.J.: Potential theory in gravity and magnetic applications. Cambridge university press. (1996).

Cembrano, J., Hervé, F. Lavenu, A.: The Liquiñe-Ofqui Fault Zone: a long-lived intra-arc fault system in southern Chile. *Tectonophysics* 256. pp. 55 – 66. (1996).

Cembrano, J., Schermer, E., Lavenu, A., Sanhueza, A.: Contrasting nature of deformation along an intra-arc shear zone, the Liquiñe–Ofqui fault zone, southern Chilean Andes. *Techtonophysics* 319. pp. 129 – 14. (2000).

Cembrano, J., and Lara, L.E.: The link between volcanism and tectonics in the southern volcanic zone of the Chilean Andes: A review: *Tectonophysics* 471. pp. 96 – 113. (2009).

Cockett, R., Kang, S., Heagy, L., Pidlisecky, A., Oldenburg, D.W.: SimPEG: An open souce framework for simulation and gradient based parameter estimation in

geophysical applications. *Computers & Geosciences* 85. pp.142 – 154. (2015).

Cox, S.: The application of failure mode diagrams for exploring the roles of fluid pressure and stress states in controlling styles of fracture-controlled permeability enhancement in faults and shear zones. *Geofluids* 10. pp. 217–233. (2010).

Glassley, W.E.: Geothermal energy. Renewable energy and the environmental. 2do edi. CRC Press. 363 p. (2015).

Harvey, C., Beardsmore, G. Moeck, I., Rüter, H.: Geothermal Exploration. Global Strategies and Applications. IGA Academy Books, Germany, FSC. 196 p. (2016).

Held, S., Schill, E., Schneider, J., Nitschke, F., Morata, D., Neumann, T., Kohl, T.: Geochemical characterization of the geothermal system at Villarrica volcano, Southern Chile; Part 1: Impacts of lithology on the geothermal reservoir. *Geothermics* 74. pp. 226 – 239. (2018).

Kana, J., Djongyang, N., Raïdandi, D., Nouck, P., Dadjé, A.: A review of geophysical methods for geothermal exploration. *Renewable and Sustainable Energy Reviews* 44. pp. 87 – 95. (2015).

Lara, L., Moreno, H.: Geología del Área Liquiñe-Neltume, Regiones de Los Lagos y de la Araucanía. Servicio Nacional de Geología y Minería. Carta Geológica de Chile, Serie Geología Básica, 83, 1. Scale 1:100.000. (2004).

Luebert, F., and Pliscoff, P.: Sinopsis bioclimática y vegetacional de Chile. Editorial Universitaria. (2006).

Meju, M.A.: Geoelectromagnetic exploration for natural resources: models, case studies and challanges. *Surveys in Geophysics* 23(2-3). pp. 133 – 206. (2002).

Melnick, D., Rosenau, M., Folguera, A., Echtler, H.: Neogene tectonic evolution of the Neuquén Andes western flank (37-39°S). *Geol. Soc. Spec. Pap.* 407. (2006).

Mickelthwaite, S., Sheldon, H., Baker, T.: Active fault and shear processes and their implications for mineral deposit formation and discovery. *Journal of Structural Geology* 32. pp. 151 – 165. (2010).

Miller, C.A., Williams-Jones, G., Fournier, D., Witter, J.: 3D gravity inversion and thermodynamic modelling reveal properties of shallow silicic magma reservoir beneath Laguna del Maule, Chile. *Earth and Planetary Science Letters* 459. pp. 14 – 24. (2017).

Munizaga, F., Herve, F., Drake, R., Pankhurst, R. J., Brook, M., and Snelling, N.: Geochronology of the Lake Region of south-central Chile (39-42 °S): Preliminary results. *Journal of South American Earth Sciences* 1(3). pp. 309 – 316. (1988).

Muñoz, G.: Exploring for geothermal resources with electromagnetic methods. *Surveys in Geophysics* 35(1). pp. 133-206. (2014).

Pérez-Flores, P., Cembrano, J., Sanchez, P., Veloso, E., Arancibia, G., Roquer, T.: Tectonics, magmatism and paleo-fluid distribution in a strike-slip setting: Insights from the northern termination of the Liquiñe-Ofqui fault System, Chile. *Tectonophysics*. pp. 192 – 210. (2016).

Rosenau, M., Melnick, D., Echtler, H.: Kinematic constraints on intra-arc shear and strain partitioning in the southern Andes between 38°S and 42°S latitude. *Tectonics* 25. pp. 1 – 16. (2006).

Rowland, J.V., Simmons, S.F.: Hydrologic, magmatic, and tectonic controls on hydrothermal flow, Taupo Volcanic Zone, New Zealand. Implications for the formation of epithermal vein deposits. *Econ. Geol*. 107. pp. 427 – 457. (2012).

Sánchez, P., Pérez-Flores, P., Arancibia, G., Cembrano, J., Reich, M.: Crustal deformation effects on the chemical evolution of geothermal systems: the intra-arc Liquiñe–Ofqui fault system, Southern Andes. *International Geology Review* 55 (11). pp. 1384 – 1400. (2013).

Tardani, D., Reich, M., Roulleau, E., Takahata, N., Sano, Y., Pérez-Flores, P., Sánchez, P., Cembrano, J., Arancibia, G.: Exploring the structural controls on helium, nitrogen and carbon isotopes composition in hydrothermal fluids along an intra-arc fault system. *Geochimica et Cosmochimica Acta*. pp. 193 – 211. (2016).

Tassara, A., and Yañez, G.: Relationship between elastic thickness and the tectonic segmentation of the Andean margin (15-47 °S). Revista Geológica de Chile 30 (2). pp. 159 – 186. (2010).

Wrage, J., Tardani, D., Reich, M., Daniele, L., Arancibia, G., Cembrano, J., Sánchez-Alfaro, P., Morata, D.: Geochemistry of thermal waters in the Southern Volcanic Zone, Chile- Implications for structural controls on geothermal fluid composition. *Chemical Geology* 466. pp. 545 – 561. (2017).